Articles

Self-Assembly of Poly(ethylene oxide)-*b*-poly(ϵ-caprolactone) Copolymers in Aqueous Solution

P. Vangeyte,[†] B. Leyh,[‡] M. Heinrich,[§] J. Grandjean,[∥] C. Bourgaux,[⊥] and R. Jérôme*,[†]

Center for Education and Research on Macromolecules (CERM), Laboratoire de Dynamique Moleculaire, and Chimie Organique et Spectroscopie Multinucléaire (COSM), University of Liège, Sart-Tilman B6a, B-4000 Liège, Belgium, Forschungszentrum Jülich, Institut für Festkörperforschung, Postfach 1913, D-52425 Jülich, Germany, and Laboratoire pour l'Utilisation du Rayonnement Electromagnétique, University of Paris-Sud, B209D, 91898 Orsay, France

Received February 4, 2004. In Final Form: June 11, 2004

The associative behavior of monodisperse diblock copolymers consisting of a hydrophilic poly(ethylene oxide) block and a hydrophobic poly(ϵ-caprolactone) or poly(γ-methyl-ϵ-caprolactone) block has been studied in aqueous solution. Copolymers have been directly dissolved in water. The solution properties have been studied by surface tension, in relation to mesoscopic analyses by NMR (self-diffusion coefficients), transmission electron microscopy, and small-angle neutron and X-ray scattering. The experimental results suggest that micellization occurs at low concentration (∼0.002 wt %) and results in a mixture of unimers and spherical micelles that exchange slowly. The radius of the micelles has been measured (ca. 11 nm), and the micellar substructure has been extracted from the fitting of the SANS data with two analytical models. The core radius and the aggregation number change with the hydrophobic block length according to scaling laws as reported in the scientific literature. The poly(ethylene oxide) blocks are in a moderately extended conformation in the corona, which corresponds to about 25% of the completely extended chain. No significant modification is observed when poly(γ-methyl-ϵ-caprolactone) replaces poly(ϵ-caprolactone) in the diblocks.

Introduction

Amphiphilic block copolymers find applications in various fields, such as detergency,[1] emulsions,[2] drug delivery systems,[3] and dispersions.[4] These copolymers are known for micellization in solvents selective for one block. Micelles are usually spherical, with a core formed by the nonsoluble blocks, surrounded by a corona of the solvated chains.[5]

Only few nonionic amphiphilic copolymers have been studied in water. The most representative ones are block copolymers of ethylene oxide (EO) and propylene oxide, known as "Pluronics".[6−14] Other copolymers associate a hydrophilic poly(ethylene oxide) (PEO) block with poly(styrene),[15] poly(oxybutylene) (PBO),[16−19] and poly(butadiene) (PB),[20] respectively. These polymeric amphiphiles were reviewed by Alexandridis in 1996.[21]

This paper deals with amphiphilic copolymers that contain a water-soluble biocompatible PEO block and a hydrophobic biodegradable poly(ϵ-caprolactone) (PCL) or poly(γ-methyl-ϵ-caprolactone) (PMCL) block. PEO-*b*-PCL

* To whom correspondence should be addressed.
[†] CERM, University of Liège.
[‡] Laboratoire de Dynamique Moleculaire, University of Liège.
[§] Institut für Festkörperforschung.
[∥] COSM, University of Liège.
[⊥] University of Paris-Sud.

(1) Jönsson, B.; Lindman, B.; Holmberg, K.; Kronberg, B. *Surfactants and Polymers in Aqueous Solution*; Wiley & Sons, Ltd.: Chichester, 1998.
(2) Piirma, I. *Polymeric Surfactants*; Marcel Dekker: New York, 1992; Chapter 4.
(3) Kataoka, K.; Harada, A.; Nagasaki, Y. *Adv. Drug Delivery Rev.* **2001**, *47*, 113.
(4) Alexandridis, P.; Lindman, B. *Amphiphilic Block Copolymers : Self-Assembly and Application*; Elsevier: Amsterdam, 2000; Chapters 13−17.
(5) Hamley, I. W. *The physics of Block Copolymers*; Oxford University Press: Oxford, 1998; Chapter 3.
(6) Lopes, J. R.; Loh, W. *Langmuir* **1998**, *14*, 750.
(7) Wanka, G.; Hoffmann, H.; Ulbricht, W. *Colloid Polym. Sci.* **1990**, *268*, 101.
(8) Linse, P. *J. Phys. Chem.* **1993**, *97*, 13896.
(9) Lin, Y.; Alexandridis, P. *J. Phys. Chem. B* **2002**, *106*, 12124.
(10) Kositza, M. J.; Bohne, C.; Alexandridis, P.; Hatton, T. A.; Holzwarth, J. F. *Macromolecules* **1999**, *32*, 5539.
(11) Goldmints, I.; Yu, G.; Booth, C.; Smith, K.A.; Hatton, T. A. *Langmuir* **1999**, *15*, 1651.
(12) Kelarakis, A.; Havredaki, V.; Yu, G. E.; Derici, L.; Booth, C. *Macromolecules* **1998**, *31*, 944.
(13) Chu, B. *Langmuir* **1995**, *11*, 414.
(14) Almgren, M.; Brown, W.; Hvidt, S. *Colloid Polym. Sci.* **1995**, *273*, 2.
(15) Xu, R.; Winnik, M. A.; Riess, G.; Chu, B.; Croucher, M. D. *Macromolecules* **1992**, *25*, 644.
(16) Yu, G.; Yang, Z.; Ameri, M.; Attwood, D.; Collett, J. H.; Price, C.; Booth, C. *J. Phys. Chem. B* **1997**, *101*, 4394.
(17) Chlebicki, J. *J. Colloid Interface Sci.* **1998**, *206*, 77.
(18) Derici, L.; Ledger, S.; Mai, S.; Booth, C.; Hamley, I. W.; Pedersen, J. S. *Phys. Chem. Chem. Phys.* **1999**, *1*, 2773.
(19) Soni, S. S.; Sastry, N. V.; Patra, A. K.; Joshi, J. V.; Goyal, P. S. *J. Phys. Chem. B* **2002**, *106*, 13069.
(20) Won, Y.; Davis, H. T.; Bates, F. S.; Agamalian, M.; Wignall, G. D. *J. Phys. Chem. B.* **2000**, *104*, 7134.
(21) Alexandridis, P. *Curr. Opin. Colloid Interface Sci.* **1996**, *1*, 490.

10.1021/la049695y CCC: $27.50
Published on Web 08/26/2004

Table 1. Composition and Molecular Weight Distribution of PEO-*b*-PCL and PEO-*b*-PMCL Block Copolymers

sample PEO_x-*b*-P(M)CL_y	M_n PEO[a]	M_n PCL[b] (or PMCL)	N_s[c]	N_c[c]	EO (mol %)	EO/CL (wt %)	polydispersity index
PEO_{114}-*b*-PCL_3	5000	350	114	3	97.5	93.5	1.10
PEO_{114}-*b*-PCL_8	5000	950	114	8	93.5	84.0	1.10
PEO_{114}-*b*-PCL_{16}	5000	1850	114	16	87.5	73.0	1.16
PEO_{114}-*b*-PCL_{19}	5000	2200	114	19	85.5	69.5	1.14
PEO_{114}-*b*-PCL_{34}	5000	3900	114	34	77.0	56.0	1.17
PEO_{114}-*b*-$PMCL_3$	5000	350	114	3	97.5	93.5	1.07
PEO_{114}-*b*-$PMCL_{12}$	5000	1500	114	12	90.5	77.0	1.12
PEO_{114}-*b*-$PMCL_{27}$	5000	3450	114	27	81.0	59.0	1.15

[a] Determined by SEC measurements with PEO standards. [b] Calculated by integration of characteristic ^{1}H NMR resonances for PEO and PCL. [c] N_s and N_c are the number of monomer units for the PEO and the PCL blocks, respectively.

has already been studied for its potential as a drug delivery system.[22,23]

Because amphiphilic copolymers may resist direct dissolution in water, water-miscible organic solvents are usually used as transient cosolvents. Copolymers are dissolved first in the organic cosolvent or in an organic solvent−water mixture, followed by water addition and elimination of the organic solvent by different methods.[24−28] Several research groups used this method to prepare PEO-*b*-PCL nanoparticles.[22,23,29,30] However, PCL-*b*-PEO-*b*-PCL triblock copolymers with very short PCL blocks (two to six monomer units) have been directly dissolved in water.[31] To the best of our knowledge, the PEO-*b*-PMCL diblocks have only been considered by our group with the purpose to prepare nanoparticles.[32]

In this work, micelles of amphiphilic PEO-*b*-PCL and PEO-*b*-PMCL block copolymers have been prepared by direct dissolution in water. Attention has been paid to the properties of these micellar solutions in the dilute regime and to the structure of the micelles taking into account the possible effect of the aggregate polydispersity. The hydrophilic−hydrophobic balance of these copolymers has been changed in series of copolymers, which differ by the length of the hydrophobic block, either crystallizable PCL or amorphous PMCL.[33,34]

Experimental Section

Copolymer Synthesis. Amphiphilic PEO-*b*-PCL and PEO-*b*-PMCL diblocks were synthesized by sequential anionic polymerization of EO followed by ring-opening polymerization of either ϵ-caprolactone (CL) or γ-methyl-ϵ-caprolactone (MCL). Briefly, EO bulk polymerization was initiated by triethyleneglycol monomethyl ether added with KOH (0.2 wt %) as a catalyst at 115 °C. After purification, the hydroxyl-terminated PEO was reacted with a trialkylaluminum, with formation of a macroinitiator for the ring-opening polymerization of CL and MCL. Polymerization was carried out at 25 °C in methylene chloride (5 wt % solution) added with 1 equiv pyridine. Copolymers were precipitated in heptane (a common nonsolvent for the two blocks) to remove unreacted monomers (CL or MCL). They were then dissolved in an 80:20 water/tetrahydrofuran (THF) mixture and purified by dialysis against water (elimination of residual PEO and Al salt), followed by lyophilization of the solution and release of a very powdery material.[35]

Size-exclusion chromatography (SEC) was carried out in THF at 40 °C with a Hewlett-Packard 1090 liquid chromatograph and a Hewlett-Packard 1037A refractometer index detector. The molecular weight of the first PEO block and the polydispersity of the copolymers were measured by SEC. The molecular weight of the second block was calculated from the molecular weight of the first block and the ^{1}H NMR spectra (Brucker AM 400 spectrometer) and the relative intensities of the PEO and PCL peaks at 3.65 and 4.06 ppm, respectively. The block copolymers used in this study are listed with their molecular characteristics in Table 1.

Preparation of Micelles. Unless otherwise stated, all the solutions were prepared as follows. Well-known amounts of lyophilized copolymer and bidistilled water (typically 10 g of water were added to 20 mg of copolymer) were mixed and heated under vigorous stirring at 82 °C for 12 min. These solutions were kept under stirring for 18 h and then at rest for 24 h before any measurement. They were used no later than 10 days after preparation. For NMR and small-angle neutron scattering (SANS) measurements, bidistilled water was replaced by D_2O (Cambridge Isotope Laboratories 99.9%), used as received.

Surface Tension. Surface tension was recorded with an automatic Krüss K12 tensiometer, equipped with a platinum Wilhelmy plate at 25 °C. The glassware was dipped in a sulfochromic acid solution for at least 6 h, thoroughly rinsed with distilled water, and dried in an oven at 50 °C. The platinum plate was cleaned with water and chloroform and flamed before each measurement. Surface tension of pure bidistilled water (72 mN/m) was measured to check the cleanness of the glassware. Each measurement of surface tension was repeated at least five times and accepted whenever the values were reproducible within 0.02 mN/m. The surface excess concentration, Γ_1 (mol/cm^2), was extracted from the higher slope of the surface tension versus concentration plot, and the surface area per molecule, a^s, was calculated from eq 1.[36]

$$a^s = 10^{16}/N\Gamma_1 \quad (1)$$

where N is the Avogadro number.

NMR Self-Diffusion Coefficients. Self-diffusion experiments were performed with a Brucker AM 300WB spectrometer operating at the proton Larmor frequency of 300 MHz at 25 °C, by the Fourier transform pulsed-gradient spin−echo (PGSE) technique. The so-called longitudinal-eddy-current delay sequence developed by Gibbs and Johnson, associated with a phase-cycling procedure adapted by Johnson, was used.[37,38] The spectrometer was equipped with a Brucker pulse magnetic field gradient unit. This sequence was chosen because echo attenuation during experiments is essentially due to T_1 relaxation, which

(22) Luo, L.; Tam, J.; Maysinger, D.; Eisenberg, A. *Bioconjugate Chem.* **2002**, *13*, 1259.
(23) Soo, P. L.; Luo, L.; Maysinger, D.; Eisenberg, A. *Langmuir* **2002**, *18*, 9996 (and references therein).
(24) Yu, Y.; Eisenberg, A. *J. Am. Chem. Soc.* **1997**, *119*, 8383.
(25) Zhang, L.; Eisenberg, A. *Sciences* **1995**, *268*, 1728.
(26) Kataoka, K.; Harada, A.; Nagasaki, Y. *Adv. Drug Delivery Rev.* **2001**, *41*, 113.
(27) De Jaeghere, F.; Allémann, E.; Feijen, J.; Kissel, T.; Doelker, E.; Gurny, R. *J. Drug Targeting* **2000**, *8*, 143.
(28) Gohy, J. F.; Creutz, S.; Garcia, M.; Mahltig, B.; Stamm, M.; Jérôme, R. *Macromolecules* **2000**, *33*, 6378.
(29) Zhao, Y.; Liang, H.; Wang, S.; Wu, C. *J. Phys. Chem. B* **2001**, *105*, 848.
(30) Kim, S. Y.; Lee, Y. M. *Biomaterials* **2001**, *22*, 1697.
(31) Martini, L.; Attwood, D.; Collett, J. H.; Nicholas, C. V.; Tanodekaew, S.; Deng, N.; Heatley, F.; Booth, C. *J. Chem. Soc., Faraday Trans.* **1994**, *90*, 1961.
(32) Vangeyte, P.; Gautier, S.; Jérôme, R. *Colloids Surf., A* **2004**, *242*, 203.
(33) Trollsas, M.; Kelly, M. A.; Claesson, H.; Siemens, R.; Hedrick, J. L. *Macromolecules* **1999**, *32*, 4917.
(34) Vion, J. M. Ph.D. Thesis, University of Liège, Liège, Belgium, 1986.
(35) Vangeyte, P.; Jérôme, R. *J. Polym. Sci., Part A: Polym. Chem.* **2004**, *42*, 1132.
(36) Rosen, M. J., Ed. *Surfactants and Interfacial Phenomena*; Wiley: New York, 1989.
(37) Gibbs, S. J.; Johnson, C. S. *J. Magn. Reson.* **1991**, *93*, 395.
(38) Wu, D.; Chen, A.; Johnson, C. S. *J. Magn. Reson.* **1995**, *115*, 260.

may be significantly slower than that due to T_2 relaxation, particularly for polymeric and colloidal systems.[39] For molecules with an unhindered Brownian motion, the decay of the echo amplitude, $A(2\tau)$ (where τ is the time between two radio-frequence pulses), for a given chemical species, obeys the Stejskal−Tanner eq 2

$$A(2\tau) = A_0 \exp[-\gamma^2 g^2 \delta^2 (\Delta - \delta/3) D] \quad (2)$$

where γ is the gyromagnetic ratio of the proton; A_0 is the initial amplitude; δ is the period of application of the magnetic field gradient, g, separated by an interval of time, Δ; and D is the self-diffusion coefficient.

Measurements were carried out at 298 K, with $\delta = 6$ ms and $\Delta = 200$ ms. The echo attenuation, A, was recorded as a function of g, from 0.204 to 4.08 T m^{-1}, and calibrated with octanol ($D = 1.9 \times 10^{-10}$ m^2 s^{-1} at 20 °C).[40] The echo attenuation for the copolymers was measured at a chemical shift of 3.65 ppm (characteristic of EO) and fitted by either a monoexponential or a biexponential function, leading to either one or two self-diffusion coefficients, D (eq 2).

From the D values, the size of the diffusing particles can be estimated by the Stokes−Einstein relationship (eq 3) on the assumption that micelles are spherical

$$D = kT/(6\pi\eta r_h) \quad (3)$$

where k is the Boltzmann's constant, T is the temperature, and η is the solvent viscosity. r_h is the so-called hydrodynamic radius of the scatterers.

All reported values are the average of three independent measurements.

Transmission Electron Microscopy (TEM). TEM was performed with a Phillips CM 100 microscope operating at an acceleration voltage of 100 kV. A drop of an aqueous solution of the copolymer to be observed (0.1 wt %) was deposited onto a Formvar-coated copper grid. Water was allowed to evaporate, at room temperature and atmospheric pressure. Finally, the samples were stained by an aqueous solution of phosphotungstic acid (0.085 w/w %). The shape and size of the copolymer assemblies were directly observed and determined.

SANS and Small-Angle X-ray Scattering (SAXS). SANS experiments were performed at the FRJ-2 reactor of the Forschungszentrum Jülich (Germany), on the KWS-1 instrument at a neutron wavelength of 7 Å, with a resolution, $\Delta\lambda/\lambda$, of 0.2 and a beam cross section of 8×8 mm^2. Two sample-to-detector distances, 8 and 2 m, respectively, allowed two ranges of scattering vectors to be covered, that is, $q = 0.006-0.04$ Å^{-1} and $q = 0.02-0.15$ Å^{-1}. The collimation distances were 8 and 4 m, respectively. The data were recorded on a two-dimensional area detector of 60×60 cm^2 with a space resolution of 0.8×0.8 cm^2. Radial averaging led to a one-dimensional scattering function $I(q)$. Solutions were analyzed in quartz cells with a 2-mm path length. Corrections for the background and sample holder contributions were carried out according to standard data handling procedures. Polymer solutions and pure solvent (D_2O) were treated in the same way, and the scattering intensities were converted to macroscopic scattering cross sections per unit volume, $d\Sigma/d\Omega$ (cm^{-1}), by using calibration with low-density polyethylene (LUPOLEN). The polymer contribution was determined by subtracting the solvent cross section weighted by its volume fraction.

SAXS experiments were carried out at the LURE-DCI Synchrotron Radiation Source at Orsay (France), on the D24 beam line equipped with a Ge(111) crystal monochromator and a linear gas detector. A wavelength, λ, of 1.49 Å was selected, and the sample-to-detector distance was 1763 mm. The q range extended from 0.011 to 0.14 Å^{-1}. The samples were contained in cells closed by Kapton windows. As for the SANS experiments, corrections were made for the background and sample holder contributions, and the solvent contribution weighed by its volume fraction was subtracted. No calibration was used to calculate absolute intensities.

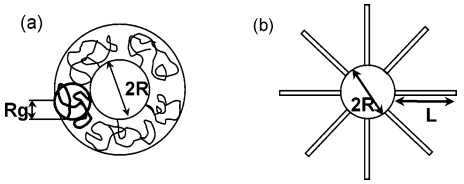

Figure 1. Models used for the form factor analysis. Each model considers a dense spherical core of radius R with either (a) Gaussian chains anchored to the core with a gyration radius R_g (Pedersen and Gerstenberg model)[48,49] or (b) rods of length L, attached at the core−shell interface.

Scattering Data Analysis. Similar procedures were used to analyze both the SANS and SAXS measurements. Here the emphasis will be on the SANS data, but most aspects are valid for both types of measurements. The low critical micelle concentration (cmc) of the amphiphilic block copolymers considered in the present paper suggests that they form micelles in the investigated concentration range (>0.2 wt %). In the framework of the decoupling approximation,[41,42] the coherent macroscopic scattering cross section ($d\Sigma/d\Omega$) of spherically symmetric micelles is proportional to the product of two factors. The first one is the form factor, $P(q)$, which describes the scattering by the individual micelles. For polydisperse micelles, the form factor has to be averaged over the micellar size distribution. The second factor, noted $S'(q)$ and often referred to as the effective structure factor, is related to the interferences between the waves scattered by different micelles.[41,42] Two experimental approaches were used to infer the micellar structure. At concentrations as low as 0.2 wt %, the intermicellar distance is large compared to the micellar radius. In the q range of interest, the effective structure factor is, therefore, equal to unity, and the small-angle scattering signal is controlled by the micellar form factor only. At larger concentrations, from 2 to 10 wt %, peaks of $S'(q)$ show up, from which information on the intermicellar distance can be extracted, as discussed later.

(a) Low Concentration Regime (0.2−0.5 wt %). Most of our SANS measurements were performed with dilute solutions in D_2O (0.2 and 0.5 wt %). D_2O was chosen to maximize the coherent scattering while minimizing incoherent scattering. Two models were found relevant to describe the micellar form factor that governs the data obtained from these experiments.[43−47] The first model, called henceforth the core−Gaussian chains model, was developed by Pedersen and Gerstenberg.[45,46] It assumes a dense hydrophobic core, of radius R, to which hydrophilic Gaussian chains characterized by their statistical segment length, b (Kuhn segment), or, equivalently, by their radius of gyration, R_g, are attached (Figure 1a). The number of Gaussian chains equals the micellar aggregation number, N_{agg}. The second model, referred to as the core−rigid rods model,[44] will be described in detail elsewhere.[47] The hydrophobic core is described in the same way as for the core−Gaussian chains model, but the N_{agg} hydrophilic corona chains are treated as rigid rods with an effective length equal to L (Figure 1b). This length gives information about the extension of the solvated hydrophilic chains in the corona.

The micellar size distribution needs to be taken into account. Because the copolymer chain polydispersity is low (see polydispersity indices in Table 1), the micellar size dispersion is assumed to derive entirely from the distribution of the aggregation number. In both models, this polydispersity manifests itself by a distribution of the core radii, $\tilde{P}(R)$. In addition, modification in the chain density within the corona by changing N_{agg} most probably

(39) Abrahmsen-Alami, A.; Persson, K.; Stilbs, P.; Alami, E. *J. Phys. Chem.* **1996**, *100*, 4598.
(40) Herden, H.; Karger, J.; Pfeifer, H.; Kube, C.; Schollner, J. *J. Colloid Interface Sci.* **1992**, *152*, 281.
(41) Pedersen, J. S.; Svaneborg, C. *Curr. Opin. Colloid Interface Sci.* **2002**, *7*, 158.
(42) Castelletto, V.; Hamley, I. W. *Curr. Opin. Colloid Interface Sci.* **2002**, *7*, 167.
(43) Yang, L.; Alexandridis, P.; Steyler, D. C.; Kositza, M. J.; Holzwarth, J. F. *Langmuir* **2000**, *16*, 8555.
(44) Fati, D. Master thesis, University of Liège, Liège, Belgium, 1999.
(45) Pedersen, J. S.; Gerstenberg, M. C. *Macromolecules* **1996**, *29*, 1363.
(46) Pedersen, J. S. *Adv. Colloid Interface Sci.* **1997**, *70*, 171.
(47) Leyh, B. To be submitted.

perturbs the corona thickness, that is, R_g or L depending on the model adopted, but in a non-straightforward way. Only the polydispersity of the aggregation number and the directly related core size distribution, $\tilde{P}(R)$, have, therefore, been taken into account. In this approach, the aggregation number dispersion affects the chain density in the corona but not the thickness. Fitting the model equations [see, e.g., eq 4 below] to the experimental data then leads to an average corona size. The core size distribution has been assumed to be Gaussian, as suggested by the TEM data that will be presented in Results.

Within this framework, the coherent macroscopic cross section (unit: length^{-1}) can be written as follows:

$$\frac{d\Sigma}{d\Omega}(q) = \frac{N}{V}\frac{(N_s b_s + N_c b_c)^2}{\langle V_{core}\rangle \tilde{v}_c}\int_0^{+\infty} \tilde{P}(R)\, V_{core}^2 P(q; R, L)\, dR \quad (4)$$

In this equation, the indices *s* and *c* stand for the hydrophobic spherical core and for the hydrophilic corona chains, respectively. N_s and N_c are the polymerization degrees of the hydrophobic and hydrophilic blocks, respectively. b_s and b_c are the corresponding excess scattering lengths of the scattering units, which correspond to monomeric units in the investigated q range. They are given by the following equation:

$$b_i = b_i' - b_{solvent}\frac{v_i}{v_{solvent}} \quad (5)$$

where b_i' and $b_{solvent}$ are the scattering lengths of the copolymer scattering units and of the solvent, respectively, and v_i and $v_{solvent}$ are the corresponding partial molecular volumes of the scatterers. $P(q; R, L)$ is the form factor (normalized to unity at $q = 0$) of a core−rods micelle with core radius R and rod length L. If the core−Gaussian chains model is adopted instead, the parameter L has to be replaced by R_g. $\langle V_{core}\rangle$ is the average volume of the hydrophobic core, whereas $\tilde{v}_s$ is the volume of a single hydrophobic chain. Finally, N/V is the number density of the copolymer chains in solution.

Note that eq 4 shows that, when $q \to 0$, $d\Sigma/d\Omega$ is proportional to $\langle V_{core}^2\rangle/\langle V_{core}\rangle$, that is, to $\langle R^6\rangle/\langle R^3\rangle$.

The analytical expression for the form factor corresponding to the core−Gaussian chains model can be found in either ref 45 or ref 46 [see, e.g., eq 74 in ref 46]. The form factor for the core−rigid rods model is given by eq 6:[44,47]

$$P(q; R, L) = \alpha_s^2\left\{\frac{3}{(qR)^3}[\sin(qR) - (qR)\cos(qR)]\right\}^2 + \frac{\alpha_c^2}{N_{agg}}\left\{\frac{2}{qL}Si(qL) - \frac{\sin^2(qL/2)}{(qL/2)^2}\right\} + 2\alpha_s\alpha_c\frac{3[\sin(qR) - (qR)\cos(qR)]}{(qR)^3}\frac{Si[q(R+L)] - Si(qR)}{qL} + \frac{\alpha_c^2}{N_{agg}}(N_{agg} - 1)\left\{\frac{Si[q(R+L)] - Si(qR)}{qL}\right\}^2 \quad (6)$$

where

$$Si(x) = \int_0^x \frac{\sin x'}{x'}\, dx'; \quad \alpha_s = \frac{N_s b_s}{N_s b_s + N_c b_c}; \quad \text{and} \quad \alpha_c = \frac{N_c b_c}{N_s b_s + N_c b_c}$$

The first term in eq 6 is the form factor for the spherical core. The second term is the sum of the thin rod form factors, whereas the last two terms are the interference cross terms between the core and the rods and between the rods themselves, respectively.

To extract the structural parameters, eq 4 is fitted to the experimental macroscopic cross sections, using a least-squares method, that consists of minimizing the squared chi (χ^2). To ensure that the global minimum of the χ^2 surface is obtained, no black box algorithm was used. A systematic mapping of the χ^2 surface as a function of R and L (core−rods model) or R_g (core−Gaussian chains model) was performed instead. A wide domain exploration of the parameters was followed by a finer mesh optimization.

Because the scattering intensity is proportional to N_{agg}^2, that is, to the square of the core volume [hence, the $V_{core}^2 \propto R^6$ factor in eq 4], larger micelles contribute substantially to the signal. The micelles that are sampled most efficiently by the neutron scattering experiments have, therefore, a core radius that corresponds to the position of the maximum of $R^6\tilde{P}(R)$. We call this radius the "most representative core radius", and we denote it as R_r. The associated aggregation number is written $N_{agg,r}$. It is equal to

$$N_{agg,r} = \frac{4/3\pi R_r^3}{\tilde{v}_s} \quad (7)$$

This "most representative aggregation number" should not to be confused with the average aggregation number, which is related to $\langle R^3\rangle$. For the most sampled micelles, the hydrophilic chain volume fraction in the corona is given by

$$\phi_{corona,r} = \frac{N_{agg,r}\tilde{v}_c}{4/3\pi[(R_r + L)^3 - R_r^3]} \quad (8)$$

$\tilde{v}_c$ is the volume of a single hydrophilic chain. If the model of Pedersen and Gerstenberg[45] is used, $\phi_{corona,r}$ is calculated with $L = (6R_g^2)^{1/2}$ and $R_g^2 = {}^1/_6 Nb^2$, where N is the number of Kuhn segments.

(b) Higher Concentration Regime (2−10 wt %). At concentrations larger than 0.5 wt %, the effective structure factor, which describes the scattering by the distribution of the micellar centers, can no longer be equated to unity in the q range sampled. The position of the first maximum, q_{max}, is related to the intermicellar distance, d, by eq 9:[48]

$$q_{max}d = 7.2 \quad (9)$$

Assuming that in a concentrated solution (2−10 wt %) spherical micelles are stacked with a compactness factor of 0.64, the micellar concentration can be deduced from the experimental peak position and compared to the copolymer concentration, leading to the aggregation number, N_{agg}. The core radius can then be estimated under the usual assumption of a dense core.[44]

Results

Preparation of Micellar Solutions. In agreement with literature data,[29−31] copolymers with a high hydrophobic content resist direct solubilization in water even at concentrations as low as 0.001 wt %. Only the PEO_{114}-*b*-PCL_3 and PEO_{114}-*b*-$PMCL_3$ copolymers are directly soluble in water at 25 °C. Whenever the other PEO-*b*-PCL and PEO-*b*-PMCL copolymers listed in Table 1 are added with water, a finely dispersed solid coexists with a clear liquid phase that contains copolymer, and the surface tension of this liquid phase is, indeed, about 51 mN/m compared to 72 mN/m for water. Upon heating the copolymer−water mixture at 82 °C,[49] complete solubilization is observed and persists when the solution is cooled to room temperature. The solubilization problem is the same whatever the hydrophobic polyester block, PCL or PMCL, for diblocks of the same composition. This observation does not give credit to a possible crystallization effect in case of the PEO-*b*-PCL copolymers. An explanation might be a kinetic effect related to a phase separation of the copolymers when the hydrophobic block is long enough. This phase separation can occur indeed when the copolymer solution is cooled before lyophilization.

(48) Waseda, Y. The Structure of Liquid Transition Metals and their Alloys. In *Liquid Metals*; Evans, R., Greenwood, D. A., Eds.; Institute of Physics: Bristol, U.K., 1976; Vol. 30, pp 230−240.

(49) Bogdanov, B.; Vidts, A.; Van Den Bulcke, A.; Verbeek, R.; Schacht, E. *Polymer* **1998**, *39*, 1631.

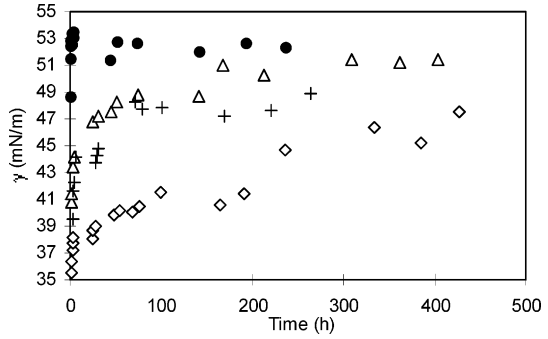

Figure 2. Time dependence of the surface tension for copolymers solution at 0.1 wt %, heated at 80 °C for 12 min without stirring: (△) PEO_{114}-*b*-PCL_8, (+) PEO_{114}-*b*-$PMCL_{12}$, (◊) PEO_{114}-*b*-PCL_{16}, and with stirring (●) PEO_{114}-*b*-PCL_{16}.

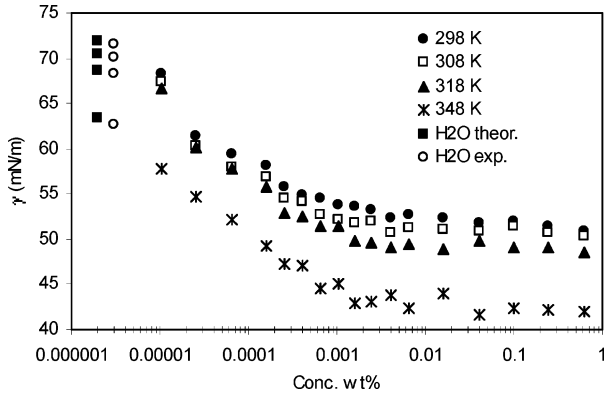

Figure 3. Surface tension of the PEO_{114}-*b*-PCL_{16} at 298 K (●) and as a function of temperature (□) 308 K, (▲) 318 K, (*) 348 K. Reference (■) and experimental (○) data for water at the same temperatures (up to down: from 298K to 348 K) are reported at a finite although low concentration, for the sake of clarity.

The time dependence of the surface tension has been measured for 0.1 wt % solutions of different P(M)CL diblocks. Figure 2 shows that the surface tension reaches about 52 mN/m at a rate that depends on the copolymer composition and stirring conditions. The time needed to reach the equilibrium surface tension increases with the length of the PCL block. Substitution of amorphous PMCL for semicrystalline PCL at a constant composition does not change the surface tension versus time plot significantly. Stirring has a very beneficial effect on the dissolution rate as exemplified by the PEO_{114}-*b*-PCL_{16} copolymer. It must be noted that no significant difference has been observed in the self-diffusion (NMR) coefficients measured for the PEO_{114}-*b*-PCL_{16} solution prepared by heating at 82 °C without stirring, for 20 and 400 h, respectively.

Aqueous solutions of the copolymers listed in Table 1 have been prepared under identical conditions, even for the diblocks with a very short P(M)CL block (three monomer units). However, the PEO_{114}-*b*-PCL_{34} copolymer could not be solubilized in water and the PEO_{114}-*b*-$PMCL_{27}$ was soluble only at concentration below 0.001 wt %. ^{1}H NMR and SEC measurements confirmed that no chain degradation occurred during the solution preparation.

Surface Tension. Surface tension of copolymer solutions of increasing concentration has been measured, as illustrated in Figure 3 for the PEO_{114}-*b*-PCL_{16} copolymer. From the γ versus concentration plot, the cmc, surface area per molecule (a^s), and γ above the cmc (γ_{cmc}) have been determined for each copolymer at 298 K as listed in Table 2. A sharp break in the experimental data at the cmc is not observed, despite a long equilibration time for each individual measurement.

Table 2. Air−Water Interface Properties of PEO_x-b-P(M)CL_y, Determined by Surface Tension Measurements

sample PEO_x-*b*-P(M)CL_y	cmc (wt %)	a^s (nm^2/molecule)	γ_{cmc} (mN/m)
PEO_{114}-*b*-PCL_3	0.1	1.02	49
PEO_{114}-*b*-PCL_8	0.0045	1.27	51
PEO_{114}-*b*-PCL_{16}	0.0015	1.12	51
PEO_{114}-*b*-PCL_{19}	0.0011	1.25	52
PEO_{114}-*b*-$PMCL_{12}$	0.0023	1.08	51
PEO_{114}-*b*-$PMCL_{27}$	*a*	1.19	53

[a] Solubility < cmc.

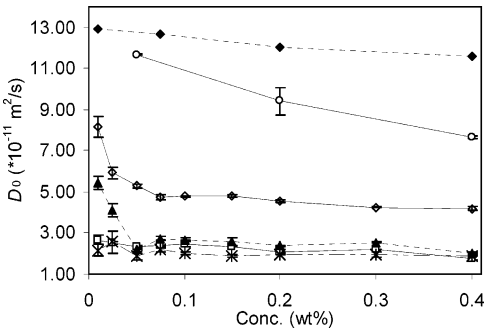

Figure 4. Concentration dependence of the self-diffusion coefficients derived from a monoexponential fitting of the NMR−PGSE experimental data for (♦) PEO, (○) PEO_{114}-*b*-PCL_3, (◊) PEO_{114}-*b*-PCL_8, (▲) PEO_{114}-*b*-$PMCL_{12}$, (□) PEO_{114}-*b*-PCL_{16}, and (*) PEO_{114}-*b*-PCL_{19}. Lines are guides for the eyes.

Micellization occurs at a low concentration (ca. 0.002 wt %), in agreement with previously reported data for PEO-*b*-PCL,[31] and for PEO-*b*-PLA (PLA = polylactide), PEO-*b*-PS, and PEO-*b*-PB of comparable molecular weight and composition.[15,16,50] The cmc decreases as the length of the hydrophobic block is increased, the effect being particularly important in the range of the shorter blocks. The cmc is decreased by 2 orders of magnitude when the degree of polymerization of the PCL block jumps from 3 to 16. The measured a^s values stay around 1.1 nm^2/molecule, which is similar to values obtained for other amphiphilic copolymers.[17,51] The variation of the surface area per copolymer with the length of the hydrophobic block is, however, not significant with respect to the experimental accuracy. The γ_{cmc}, which may be related to the surface activity, is higher than for "Pluronics" (about 35 mN/m)[12] and essentially independent of the P(M)CL block length, at least in the investigated range.

In Figure 3, the γ versus concentration plots for PEO_{114}-*b*-PCL_{16} is also reported at different temperatures. For the sake of clarity, the values for water have been plotted on the left-hand part of the figure. The change imposed on the solvent surface tension is the major effect observed. Transition at the cmc seems to be sharper at a higher temperature, without significant change in the cmc.

Self-Diffusion Coefficients. The self-diffusion coefficients (D_0) have been calculated by the monoexponential fitting of the experimental data in relation to the copolymer concentration (Figure 4). Except for the PCL_3 containing diblock (empty circles), the self-diffusion coefficient of the copolymers is basically independent of the concentration above about 0.05 wt %. Below this concentration, the self-diffusion coefficient increases with decreasing concentration as markedly as the hydrophobic block is short. Because D_0 is the average value for all the coexisting copolymer

(50) Tanodekaew, S.; Pannu, R.; Heatley, F.; Attwood, D.; Booth, C. *Macromol. Chem. Phys.* **1997**, *198*, 927.
(51) Thibaut, A. Ph.D. Thesis, University of Liège, Liège, Belgium, 2000.

Table 3. Comparison of the PEO_x-*b*-PCL_y Micellar Sizes Derived from the Different Techniques

	NMR−PGSE			TEM		SANS					
						P(*q*)				*S*(*q*)	
	r_0[a] (nm)	r_1[b] (nm)	r_2[c] (nm)	*r* (nm)	σ[d] (nm)	$R_r + L$ (nm)	*L* (nm)	R_r (nm)	$N_{agg,r}$	R_0 (nm)	N_{agg}
PEO	1.56										
PEO_{114}-*b*-PCL_3	2.13			9.37	1.75	9.46	8.3	1.12	12		
PEO_{114}-*b*-PCL_8	4.28	1.83	9.37	10.12	2.30	11.78	9.3	2.5	48	2.4	39
PEO_{114}-*b*-$PMCL_{12}$	8.87	1.95	12.46			11.83	8.1	3.7	102		
PEO_{114}-*b*-PCL_{16}	10.07	2.46	14.77			12.5	8.5	3.9	99		
PEO_{114}-*b*-PCL_{19}	8.15	1.91	12.06	10.38	1.83	11.38	6.8	4.6	126	4.26	94

[a−c] Size calculated by the Stokes−Einstein equation (eq 3) from (a) the monoexponential fit and (b,c) the biexponential fit of the experimental data. [d] Calculated as the square root of the second centered moment.

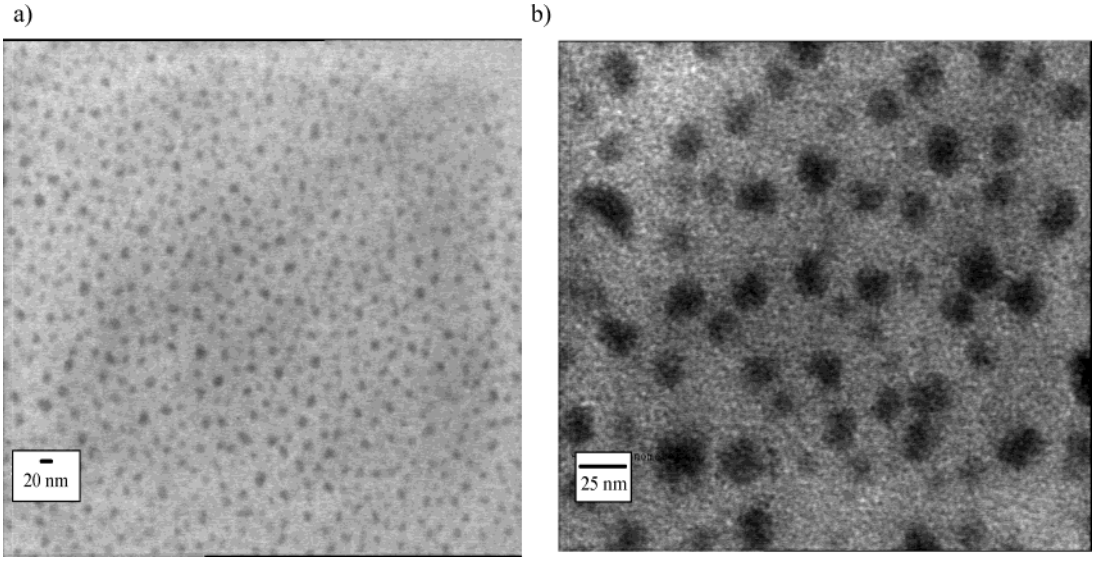

Figure 5. Micelles observed by TEM for (a) PEO_{114}-*b*-PCL_8 and (b) PEO_{114}-*b*-PCL_{16} (starting with 0.1 wt % aqueous solutions).

species, that is, unimers, micelles, aggregates, and so forth, this observation is in line with a higher content of unimers, with a self-diffusion coefficient as close to PEO as the PCL content is low.

The experimental data have also been fitted to a biexponential function. No fitting is possible in the case of PEO (no micellization) and the PEO_{114}-*b*-PCL_3 copolymer that shows a comparatively high cmc (0.1 wt %; Table 2). One type of diffusing species would, thus, dominate in solution.[52] In contrast, the fitting is good, even better, than to the monoexponential function (not shown here) for the other block copolymers. Slow (D_2) and fast (D_1) self-diffusion coefficients (large and small species) have been accordingly extracted, which are largely independent of concentration (above 0.05 wt %), within the limits of experimental errors.

The hydrodynamic radii, calculated by the Stokes−Einstein equation, are reported in Table 3. r_0, r_1, and r_2 have been calculated from D_0, D_1, and D_2, respectively. r_0 is expectedly intermediate between r_1 and r_2. Although r_1 (small species) is independent of the size of the hydrophobic block, r_0 and r_2 increase with N_b, the number of monomer units per hydrophobic block, according to the following scaling laws: $r_0 \propto N_b^{0.87}$ and $r_2 \propto N_b^{0.48}$. Again, substitution of PMCL for PCL in the diblocks has no effect.

TEM. The PEO-*b*-PCL micelles have been observed by TEM for three PCL block lengths (degree of polymerization = 3, 8 and 16 monomer units, respectively). Figure 5 compares the PEO_{114}-*b*-PCL_8 and PEO_{114}-*b*-PCL_{16} copolymers at different magnifications. Figure 5a illustrates the homogeneity of the sample (and, thus, of the parent solution). Figure 5b emphasizes the spherical shape of the micelles and the absence of secondary aggregates. Because of a limited resolution, unimers cannot be visualized by TEM. The average size and distribution parameters for the micelles observed by TEM are reported in Table 3. Histograms are also shown in Figure 6, together with the normal Gaussian distribution calculated from the standard deviations of TEM data. Note that these standard deviations refer to the global micellar radius.

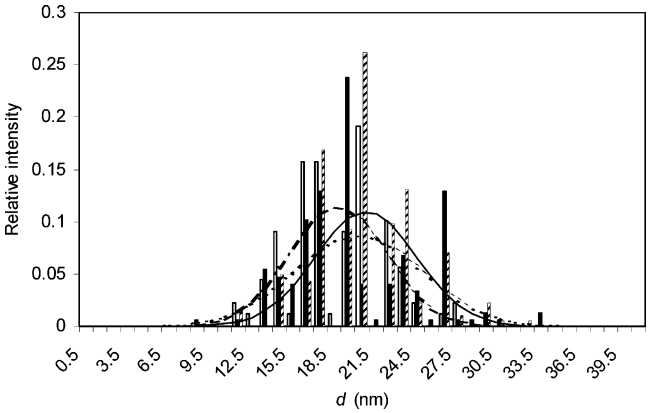

Figure 6. Size distribution measured by TEM: bars correspond to experimental data for (empty bars) PEO_{114}-*b*-PCL_3, (full bars) PEO_{114}-*b*-PCL_8, and (striped bars) PEO_{114}-*b*-PCL_{19}. Lines show the distribution calculated on the assumption of a normal distribution: dotted (PEO_{114}-*b*-PCL_8), broken (PEO_{114}-*b*-PCL_3), and continuous (PEO_{114}-*b*-PCL_{19}) lines.

SANS. The internal structure of the copolymer micelles has been made available by neutron scattering. Figure 7

(52) Hakansson, B.; Nyden, M.; Söderman, O. *Colloid Polym. Sci.* **2000**, *278*, 399.

Table 4. Structural Parameters of the Micelles According to the Two Models Used To Fit the SANS Scattering Cross Sections for PEO_x-*b*-PCL_y in D_2O

copolymer	fit[a]	R_r (nm)	L (nm)	R_g (PEO) (nm)	b (nm)	$\langle R^2\rangle^{1/2}$ (nm)	$N_{agg,r}$	$\phi_{corona,r}$	A_c (nm^2)
PEO_{114}-*b*-PCL_3	1	0.88		3.45	1.41	8.45	6	0.01	1.62
	2	1.12	8.34				12	0.02	1.31
PEO_{114}-*b*-PCL_8	1	2.18		3.47	1.42	8.50	32	0.04	1.87
	2	2.51	9.27				48	0.05	1.65
PEO_{114}-*b*-$PMCL_{12}$	1	3.74		3.03	1.08	7.42	101	0.12	1.74
	2	3.75	8.08				102	0.10	1.73
PEO_{114}-*b*-PCL_{16}	1	4.02		3.18	1.19	7.79	102	0.02	1.99
	2	3.98	8.53				99	0.09	2.01
PEO_{114}-*b*-PCL_{19}	1	4.67		2.65	0.83	6.49	134	0.17	2.04
	2	4.58	6.80				126	0.15	2.09

[a] Fits 1 and 2 correspond to the core−Gaussian chains and the core−rods models, respectively.

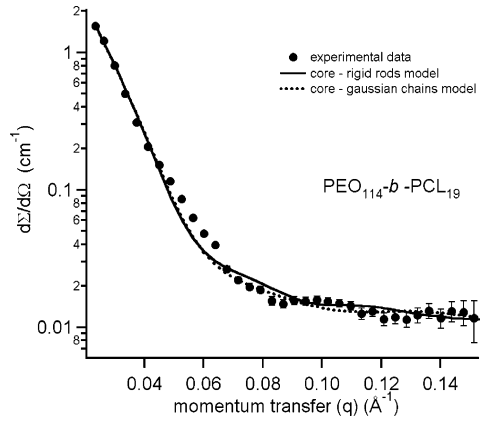

Figure 7. Comparison of the two models considered in the fitting process for the SANS form factor of the PEO_{114}-*b*-PCL_{19} copolymer (0.2 wt %).

compares the two models described in Scattering Data Analysis, for the PEO_{114}-*b*-PCL_{19} diblock. The quality of the fits is unfortunately not very sensitive to the standard deviation, σ, of the core radius distribution, $\tilde{P}(R)$, provided σ is larger than 0.2 nm. It is, therefore, not possible to extract the width of the $\tilde{P}(R)$ distribution from our data. The standard deviation has then been fixed at 0.5 nm. We must emphasize that the most sampled core radius, R_r, and the corona thickness, L, vary only slightly, when σ is increased. As an example, for PEO_{114}-*b*-PCL_8, increasing σ from 0.2 to 1.0 nm changes R_r by 0.2 nm and L by 0.45 nm, that is, a relative variation of less than 8% for both the parameters.

The fitting procedure to eq 4 calls for some additional explanation. Because the copolymer concentration, N/V, the degrees of polymerization of each block, N_s and N_c, and the excess scattering lengths, b_s and b_c, are known, it is possible to fit eq 4 to the absolute macroscopic cross sections. The two major structural parameters, the core and corona sizes, govern both the rate of decrease of the cross section as a function of q and the absolute intensity. Because systematic errors in the calibration procedure can affect $d\Sigma/d\Omega$, data have also been fitted to the relative scattering intensity, which is proportional to $\langle V_{core}\rangle^{-1}\int_0^{+\infty} \tilde{P}(R)\ V_{core}^2 P(q;\ R,\ L)\ dR$ [see eq 4]. The proportionality constant is then left as a free parameter. As a rule, the two procedures give similar core sizes within 10%. The corona thickness is observed to be larger by 10 to 20% in the case of a fit to the absolute cross sections, because of a preferential weighing of the low q range. The relative intensity variation is thought, however, to be more robust information than the absolute intensities, which can be biased by systematic errors.

The results of the fitting procedure to the relative intensities are summarized in Table 4. Data for the PEO_{114}-*b*-$PMCL_{12}$ copolymer with a hydrophobic PMCL block are consistent with the series of the PCL-containing diblocks.

As a rule, the two models for the form factor are in good agreement (Figure 7). On the basis of the χ^2 criterion, which on average is 10−20% lower for the core−rods model, the latter should be slightly favored, except for the PEO_{114}-*b*-PCL_3 copolymer with the shortest hydrophobic block. The experimental data have also been fitted to the spherical core−shell model.[43,46] The core and corona sizes extracted by this lower quality fit are in qualitative agreement with the two other models. Slightly smaller sizes are, however, systematically observed.

From the position of the $S(q)$ peaks in the scattering profiles for concentrated solutions, the average aggregation number and the average core radius for a dense spherical core have been calculated. Results for the PEO_{114}-*b*-PCL_{19} and PEO_{114}-*b*-PCL_8 copolymers are reported in Table 3. The data have been extrapolated to zero concentration. R_0 and $N_{agg,0}$ values are in good agreement with the analysis at lower concentration.

The results of the fits to the core−Gaussian chains model call for three comments. First, the Kuhn segment obtained, $b = 1.2 \pm 0.2$ nm, is larger than the value reported in the scientific literature for homo-PEO (0.77−0.79 nm)[53] and for "Pluronics P85" (1.0 nm), which indicates that the PEO blocks are more rigid in the PEO-*b*-PCL copolymers. Second, the root-mean-square distance between the chain ends, $\langle R^2\rangle^{1/2}$, is close to L obtained for the core−rods model (Table 4), which confirms that the PEO chains have a noticeable extension. Finally, even though the signal at large q is not intense enough to allow a very reliable determination of the asymptotic behavior, it is nevertheless observed to scale to $q^{-1.1\pm0.3}$ between 0.09 and 0.14 Å^{-1}, which is consistent with rod-shaped (one-dimensional) objects. This indicates that the Pedersen and Gerstenberg model[45] gives credit to somewhat extended Gaussian chains which can alternatively be described as rods.

The structural parameters calculated by the core−rods model have been plotted against the number of monomer units in the hydrophobic block, N_s (Figure 8). These data obey the following scaling relationships: $R_r \propto N_s^{0.77\pm0.05}$, $N_{agg,r} \propto N_s^{1.29\pm0.13}$, and $(R_r + L) \propto N_s^{0.12\pm0.04}$. The core and corona sizes have also been inserted in eq 10, derived from a theoretical model by Nagarajan,[54] to extract the interaction parameter between the corona (PEO) and the solvent, $\chi_{cw} = \chi_{PEO-D_2O}$, as a function of the PEO volume fraction in the corona, given for each copolymer composition by eq 8:

$$\frac{L}{R_r} = 0.867\left[\frac{1}{2} + \frac{N_s^2 N_c}{(N_s + N_c)^3} - \chi_{cw}\right]^{1/5} N_s^{-8/11} N_c^{6/7} \quad (10)$$

(53) Herman, M. F. *Macromolecules* **2001**, *34*, 4580.
(54) Nagarajan, R.; Ganesh, K. *J. Chem. Phys.* **1989**, *90*, 5843.

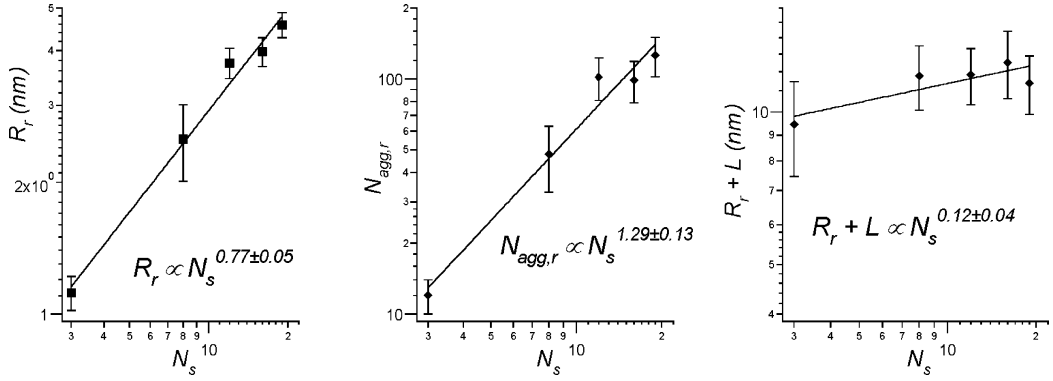

Figure 8. Core radius (left), aggregation number (middle), and global micellar size (right) of copolymer micelles as a function of the number of hydrophobic monomer units, N_s. Data derived from SANS experiments.

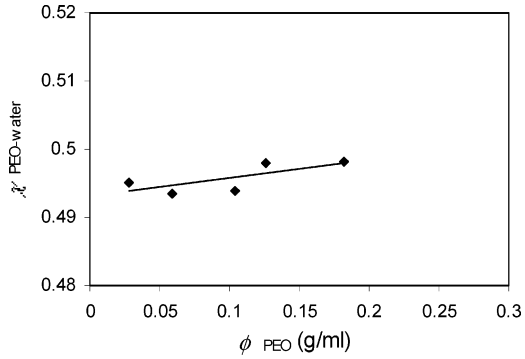

Figure 9. Dependence of the water−PEO interaction parameter, $\chi_{water-PEO}$, on the PEO concentration in the shell.

The results are displayed in Figure 9. The average χ_{PEO-D_2O} value of 0.495 is consistent with literature data.[15]

SAXS. The scattering data at a low concentration have been fitted to the core−rods model. Polydispersity was again taken into account by a Gaussian core radius distribution with a 0.5-nm standard deviation. R_r values are in reasonable agreement with SANS results, whereas L values are larger. The discrepancy between SAXS and SANS becomes larger for shorter hydrophobic blocks, because of the small scattering intensity detected for such copolymers. The core radius is found to scale to $N_b^{1.0\pm0.2}$ in a fair agreement with the SANS measurements.

Structure factors measured for concentrated solutions show the same concentration dependence as in neutron scattering experiments. The extrapolation to zero concentration confirms the values of the core radius provided by the analysis of the form factor, except for the weakly scattering PEO_{114}-*b*-PCL_3 copolymer.

Discussion

Amphiphilic block copolymers strongly differ from classical surfactants by the dynamics of the unimer−micelle equilibrium.[55−57] Figure 2 shows that the surface tension of copolymer solution (0.1 wt %) in water reaches a plateau value as slowly as the size of the hydrophobic block is large (at a constant length of the hydrophilic block), which is consistent with a shift in the unimer−micelle equilibrium toward micelles and with a slower rate of exchange.

Direct dissolution of amphiphilic copolymers in water with the assistance of temperature has been previously reported for poly(styrene) (PS)-*b*-poly(sodium acrylate) (heating at 100 °C for 80 h)[58] and PS-*b*-PEO (1 h at 65 °C).[15] At a high temperature, the hydrophobic chains become mobile enough for micelles to be formed and to participate in an unimer−micelle exchange. The solution properties are then independent of further heating;[55,56] they only depend on the way the system self-organizes during cooling. In this work, the same situation prevails, and substitution of amorphous PMCL for semicrystalline PCL has no effect on the experimental results, all the other conditions being identical. Moreover, wide-angle X-ray scattering experiments conducted with a solution of PEO_{114}-*b*-PCL19 show no crystalline peak. All these observations suggest that PCL, which is melted at 82 °C in water, does not crystallize in the micellar core when the aqueous solution is cooled to room temperature. Cores of PCL and PMCL blocks of the same length have, thus, the same characteristic features.

Figure 2 shows that the time dependence of the surface tension of the copolymer solutions is controlled by the length of the hydrophobic block at a constant length of PEO. The reason has to be found in the proportion of the free chains and their mobility, which decrease with the increasing size of the polyester block.

Surface tension data as a function of concentration show a broad transition at the cmc. This transition was discussed by Linse and Hatton in the case of "Pluronics".[59] They observed a broadening of the transition at the cmc when the copolymer polydispersity is considered in the model. They pointed out that the preferential adsorption at low concentration of more surface-active copolymer chains with a larger hydrophobic block was responsible for poor accuracy on the determination of cmc and surface excess concentration (see also Rippner et al.).[60] Alexandridis et al. observed the same phenomenon and argued that a molecular rearrangement occurs before micellization, which accounts for the transition broadening and, in some cases, for two transitions.[59−61] Measurements at higher temperature were helpful to clear up the origin of the two underlying transitions. The concentration at which the molecular rearrangement occurs changes with temperature. In this study, the temperature dependence of the surface tension versus concentration plot for the PEO_{114}-*b*-PCL_{16} copolymer is in favor of a single broad transition. As the temperature is increased, the transition becomes sharper, more likely because of the known decrease of the PEO solubility, as discussed by Jain and Malmsten.[57,62]

(55) Smith, C. K.; Liu, G. *Macromolecules* **1996**, *29*, 2060.
(56) Van Stam, J.; Creutz, S.; De Schrijver, F. C.; Jérôme, R. *Macromolecules* **2000**, *33*, 6388.
(57) Malmsten, M.; Lindman, B. *Macromolecules* **1992**, *25*, 5440.
(58) Khougaz, K.; Astafieva, I.; Eisenberg, A. *Macromolecules* **1995**, *28*, 7135.
(59) Linse, P.; Hatton, T. A. *Langmuir* **1997**, *13*, 4066.
(60) Rippner, B.; Boschkova, K.; Claesson, P. M.; Arnebrant, T. *Langmuir* **2002**, *18*, 5213.
(61) Alexandridis, P.; Athanassiou, V.; Fukuda, S.; Hatton, T. A. *Langmuir* **1994**, *10*, 2604.

Moreover, no significant evolution in the cmc is observed as was reported by Booth and Attwood for EO−butylene oxide block copolymers.[12] The authors explained this athermal micellization by the hydrophobicity of the [poly(butylene oxide)] block that would already be coiled in the monomolecular micelles (unimers). This explanation can be extended to the hydrophobic PCL and PMCL blocks in this work.

The echo attenuation recorded when the copolymer solutions are analyzed by PGSE does not fit well to a monoexponential function, as is usually observed in cases of gelation, restricted diffusion, secondary aggregation, and polydispersed systems.[39,63] Gelation and hindered diffusion can be precluded in the dilute regime investigated in this study. Moreover, no secondary aggregates have been observed by TEM. Therefore, heterogeneity of the micellar solutions is suggested to be responsible for the diffusion behavior. This heterogeneity might result from the coexistence of unimers and micelles, as suggested by Nyström et al. in the case of Pluronics,[64] in addition to polydispersity of the micelles. Although TEM and SANS cannot detect unimers unambiguously, NMR analysis provides arguments in their favor. Indeed, the self-diffusion coefficient, D_0, an average of D_1 and D_2, slightly increases when the copolymer concentration is decreased close to the cmc. It also increases when the hydrophobic block length decreases at a constant PEO block. Finally, the biexponential analysis is not applicable to PEO (no micellization) and PEO_{114}-*b*-PCL_3 (unimers are preferred consistent with a high cmc). An unimers−micelles equilibrium is, thus, quite reasonable with a shift toward micelles (thus, lower D values) when both the PCL content of the copolymers ($N_s = 8$ and higher) and the copolymer concentration are increased. The exchange rate on the NMR time scale would be slow enough for the two major species to be identified.[39]

Table 3 shows that the micellar sizes determined by the different techniques are consistent. Neutron scattering and TEM data are in good agreement, average sizes being systematically (slightly) smaller by TEM analysis. Treatment of the NMR−PGSE data leads to a constant value of r_1, close to r_0 for PEO and the expected radius of gyration of the unimers, which suggests that the two regimes observed by these NMR experiments, D_1 and D_2, correspond to unimers and micelles, respectively. The experimental values of r_1 are indeed consistent with sizes reported in the scientific literature for homo-PEO_{114} (1.56 nm) and for non-associated copolymer chains [1.5 nm for PEO_{90}-*b*-PBO_{10},[18] 2 nm for PEO_{78}-*b*-PLA_{14},[50] or 2.9 nm for Pluronics F88 (PEO_{97}-*b*-PPO_{39}-*b*-PEO_{97})].[65−67] Moreover, an estimation of the radius of gyration of the free copolymer chains taking excluded volume effects into account leads to values close to 2 nm. In this scenario, r_2 values would be average micellar radii, which are actually very close to TEM and SANS data for the micelles.

Comparison of the SANS cross sections to the core−Gaussian chains and to the core−rods models confirms the spherical shape of the micelles and provides information on the size of both the core and corona (Table 4). Deviations from the core−rods model are noticeable in the case of the PEO_{114}-*b*-PCL_3 diblock, possibly because the micelles coexist with a too large amount of unimers. As predicted by the scaling and mean-field theories,[5,54,68−70] the structural parameters of the micelles change with the length of the hydrophobic block (N_s) at a constant and much larger PEO block ($N_c \gg N_s$). The experimental scaling laws (see Figure 8) are consistent with the scaling relationships for the PEO-*b*-PPO copolymers calculated by the mean-field theory by Nagarajan and Ganesh,[54] that is, $R \propto N_s^{0.73}$, $N_{agg} \propto N_s^{1.19}$, and $(R + L) \propto N_s^{0.06}$. In contrast to other predictions,[68−70] these authors have considered the important role of the solvent-compatible block interaction. This effect becomes predominant in micellization whenever the solvent−polymer interaction is strong, as is the case for the PEO−water system (see below). The core radius and the aggregation number clearly decrease with decreasing N_s, whereas the total size ($R_r + L$) changes only slightly with the length of the hydrophobic block. The decrease of the core radius is, thus, counterbalanced by the extension of the PEO chains as N_s decreases, at least when the aggregation number is not too low.

Because of steric hindrance at the core−corona interface, the PEO chains are moderately stretched (on average, ∼25% of the totally extended chain). This extension is consistent with the low area, A_c, available to the PEO chains at the core surface ($A_c = 4\pi R_r^2/N_{agg,r}$; Table 4), compared to R_g^2. Zhang and Eisenberg[71] defined a parameter $\sigma' = a^2/A_c$, where a is the length of the repeat unit (2.85 Å for EO),[72] and they showed that chains in the corona have to adopt an extended conformations when $\sigma' N_c^{6/5} > 1$. In this study, $\sigma' N_c^{6/5}$ ranges from 11.4 (PEO_{114}-*b*-PCL_{19}) to 18.8 (PEO_{114}-*b*-PCL_3), which confirms a larger extension of the PEO chains for the diblocks with the shorter PCL blocks. This behavior is also consistent with the decrease of the PEO volume fraction, $\phi_{corona,r}$ [eq 8], when N_s decreases (Table 4). From the molecular volume of 64.6 Å^3 for one EO unit and 30 Å^3 for one water molecule,[20] the EO molar fraction in the corona is estimated to lie between 1.2×10^{-2} for PEO_{114}-*b*-PCL_3 and 8×10^{-2} for PEO_{114}-*b*-PCL_{19}, which confirms the large amount of water in the corona.

Moreover, the low volume fraction of PEO in the corona, $\phi_{corona,r}$ (<0.15), points out the high degree of swelling of the corona. The PEO-heavy water interaction parameter, χ_{PEO-D_2O}, calculated from the core−rods fit, leads to a value (0.495) in good agreement with the scientific literature (0.47; ref 15 and references therein).

Conclusions

Amphiphilic PEO-*b*-PCL and PEO-*b*-PMCL diblocks that consist of a long PEO block (degree of polymerization = 114) and a shorter polyester block [P(M)CL] of various lengths have been directly dissolved in water at 82 °C under vigorous stirring. Clear homogeneous solutions have been accordingly prepared up to high concentrations (5 wt %). The amphiphilic PEO-*b*-P(M)CL self-assemble in a progressive manner, over a large concentration range, as demonstrated by surface tension measurements. NMR self-diffusion experiments confirm that unimers coexist in solution with micelles and that the exchange occurs slowly on the NMR time scale. Spherical micelles are formed with a mean diameter of 22 nm, thus, smaller than in the case of preparation with an organic cosolvent (30−100 nm).[13] The SANS data analysis provides a deeper insight into the micellar structure. The form factors have

(62) Jain, N. J.; Aswal, V. K.; Goyal, P. S.; Bahadur, P. *J. Phys. Chem. B* **1998**, *102*, 8452.
(63) Thuresson, K.; Nilsson, S.; Kjoniksen, A. L.; Walderhaug, H.; Lindman, B.; Nyström, B. *J. Chem. Phys.* **1999**, *103*, 1425.
(64) Nyström, B.; Kjoniksen, A. L. *Langmuir* **1997**, *13*, 4520.
(65) Cau, F.; Lacelle, S. *Macromolecules* **1996**, *29*, 170.
(66) Brown, W.; Schillen, K.; Hvidt, S. *J. Phys. Chem.* **1992**, *96*, 6038.
(67) Mortensen, K.; Brown, W. *Macromolecules* **1993**, *26*, 4128.
(68) Zhulina, Y. B.; Birshtein, T. M. *Polym. Sci. U.S.S.R.* **1985**, *27* (3), 570.
(69) Halperin, A. *Macromolecules* **1987**, *20*, 2943.
(70) Whitmore, M. G.; Noolandi, J. *Macromolecules* **1985**, *18*, 657.
(71) Zhang, L.; Eisenberg, A. *J. Am. Chem. Soc.* **1996**, *118*, 3168.
(72) Tasaki, K. *J. Am. Chem. Soc.* **1996**, *118*, 8459.

been analyzed according to two main models, that is, a core−Gaussian chains[27,28] model and a core−rods model, taking the micellar size distribution into account. This analysis shows that the core radius and the aggregation number decrease with decreasing hydrophobic block length, in agreement with the scaling law predicted, for example, by Nagarajan and Ganesh.[36] This information has been confirmed by the structure factor analysis and by the SAXS measurements. Moreover, the PEO chains adopt a moderately extended conformation in the corona, as a result of the small surface area available at the core−corona interface. This chain extension in addition to a decreasing aggregation number compensates the decrease of the core radius, such that the micellar size is only slightly dependent on the hydrophobic block length. The Flory interaction parameter, $\chi_{PEO-water}$, between water and PEO has been estimated at 0.49 in agreement with the scientific literature.

Acknowledgment. The authors are very much indebted to the "Fonds pour la Formation à la Recherche dans l'Industrie et l'Agriculture" (F.R.I.A.) for a fellowship to P.V., to the "Belgian Science Policy" for financial support to CERM in the frame of the "Interuniversity Attraction Poles Program (PAI V/03)", and to the European Community -Access to Research Infrastructures action of the Improving Human Potential program (HPRI)- for financial support and access to facilities at the Forschungszentrum Jülich ("Jülich Neutrons for Europe") and of Lure (Saclay). B.L. is indebted to the F.N.R.S. (Belgium) for its financial support. The authors also thank Dr. G. Broze (Colgate-Palmolive, Liège) for surface tension measurements and V. Collard for technical assistance.

LA049695Y